Open Journal of Fluid Dynamics, 2013, 3, 92-99
http://dx.doi.org/10.4236/ojfd.2013.32A015 Published Online July 2013 (http://www.scirp.org/journal/ojfd)

Heat Transfer Enhancement of Cu-H_2O Nanofluid with Internal Heat Generation Using LBM

Mohammad Abu Taher[1], Yeon Won Lee[2], Heuy Dong Kim[1*]
[1]School of Mechanical Engineering, Andong National University, Andong, South Korea
[2]School of Mechanical Engineering, Pukyong National University, Busan, South Korea
Email: *kimhd@anu.ac.kr

Received June 10, 2013; revised June 17, 2013; accepted June 27, 2013

ABSTRACT

Fluid flow and heat transfer analysis of Cu-H_2O nanofluid in a square cavity using a Thermal Lattice Boltzmann Method (TLBM) have been studied in the present work. The LBM has built up on the D2Q9 model and the single relaxation time method called the Lattice-BGK (Bhatnagar-Gross-Krook) model. The effect of suspended nanoparticles on the fluid flow and heat transfer analysis have been investigated for different non dimensional parameters such as particle volume fraction (φ) and particle diameters (d_p) in presence of internal heat generation (q) of nanoparticles. It is seen that flow behaviors and the average rate of heat transfer in terms of the Nusselt number (Nu) as well as the thermal conductivity of nanofluid are effectively changed with the different controlling parameters such as particle volume fraction ($2\% \le \varphi \le 10\%$), particle diameter (d_p = 5 nm to 40 nm) with fixed Rayleigh number, Ra = 10^5. The present results of the analysis are compared with the previous experimental and numerical results for both pure and nanofluid and it is seen that the agreement is good indeed among the results.

Keywords: Nanofluid; Lattice-Boltzmann; Volume Fractions; Particle Diameter; Heat Generation

1. Introduction

The term nanofluid is envisioned to describe a solid-liquid mixer which consists of nano-sized solid particles and a base liquid and this is one of new challenges for thermo-sciences provided by the nanotechnology. It has potential applications in the microelectromechanical systems (MEMS) and electronics cooling industries. Therefore, in the recent years, the micro and nano systems have become of great interest due to their important and promising applications in various fields. As a result, the research topic of nanofluids has been receiving increased attention worldwide. In fact, numerous theoretical and experimental studies of the effective thermal conductivity of suspensions that contains solid particles have been conducted since Maxwell's theoretical work was published more than 100 years ago. All of the studies on thermal conductivity of suspensions have been considered with millimeter to micrometer sized particles. The use of the conventional millimeter and micrometer-sized particles in heat transfer fluids in practical devices is greatly limited by the tendency of such particles to settle rapidly and to clog mini and micro channels. Until now, it is very difficult to solid particles from eventually settling out of suspension because of particle size. However, nanoparticles appear to be ideally suited for applications in which fluids flow through small passages, because the nanoparticles are stable and small enough not to clog flow passage. Therefore, the main goal of nanofluids is to achieve the maximum thermal properties with the minimum possibility of particle volume fractions (less than 1%) and size of particles (less than 10 nm) by uniform dispersion and stable suspension of nanoparticles in base fluids/liquids. The performance of heat transfer of nanofluid depends on more factors such as shape of particles, the dimension of particles, the volume fractions of particle in the suspensions, and the thermal properties of particle materials [1,2]. However, significant amounts of experimental and theoretical work have been performed on buoyancy induced flow in conventional fluid [3,4]. The mechanism of nanoparticles, enhancement of heat transfer characteristics are described more detailedly in the books [5,6] and Yu *et al*. [7].

From the microscopic point of view, classical mechanics has no insight into the microstructure of the substance; however, statistical mechanics calculated the

*Corresponding author.

properties of state on the basis of molecular motions in a space, and on the basis of the intermolecular interactions. The Lattice Boltzmann equation (LBE) is one of the methods available to deal with such problems by Shan and Chen [8]. In general case, most of authors considered only mass and momentum conservation in LBM [9]. The macroscopic equations of these models correspond to the Navier-Stokes (NS) equations with ideal gas equation of state and a constant temperature. However, sometimes it is important to simulate thermal effects simultaneously with the fluid flows [10]. The more detailed thermal Lattice-Boltzmann method (TLBM) with some examples is discussed in the books written by Mohammad [11] and Succi [12].

A lattice Boltzmann model has been developed by Shan and Chen [13] to simulate the fluid flows containing multiple phases and components. It is also known as Shan-Chen (S-C) multi-component model. Using the two-component LBM, the Rayleigh-Benard convection in two and three dimensions for different cases have been studied by many researchers [14-17]. However, Buick and Gretaed [18] introduced a body force into LBM by modifying the collision function. To overcome the limitations of multi-component flows in the existing traditional computational methods, many researchers were interested to use multi-component LBM for multi-phase flows like solid-fluid mixtures [19-21]. In the present work, multi-component thermal Lattice-Boltzmann method (TLBM) is used for simulating natural convection H_2O-Cu nanofluid with Boussinesq approximation in a square cavity considering the internal heat generation effect of Cu nanoparticles. As far as we know, there is no work on nanofluid heat transfer under natural convection using TLBM with considering internal heat generation effect as well. The results of the analysis are compared with experimental and numerical data both for pure and nanofluids, and shown a relatively good agreement.

2. Formulation of the Problem

2.1. Mathematical Analysis

To ensure the model satisfies the N-S equations for a fluid under the influence of body force, multi-component Lattice-Boltzmann equation (LBE) can be written as [19]

$$\begin{aligned} & f_i^\sigma\left(x+e_i\Delta t, t+\Delta t\right)-f_i^\sigma\left(x,t\right) \\ & =-\frac{1}{\tau_m^\sigma}\left(f_i^\sigma\left(x,t\right)-f_i^{\sigma,eq}\left(x,t\right)\right) \\ & \quad +\frac{2\tau_m^\sigma-1}{2\tau_m^\sigma}\frac{D}{A_i c^2}\vec{e}_i\cdot\vec{F}^\sigma \end{aligned} \tag{1}$$

The function $f_i^\sigma\left(x,t\right)$ is the particle distribution function of σ = 1, 2 components with lattice velocity vectors e_i, A_i is the adjustable coefficient, D is the dimension, F^σ is applied force, and $\omega^\sigma = 1/\tau_m^\sigma$ is the relaxation parameter that depends on the local macroscopic variables ρ and $\rho\boldsymbol{u}$. These variables should satisfy the following laws of conservation:

$$\rho^\sigma\left(x,t\right)=\sum_i m^\sigma f_i^\sigma\left(x,t\right)$$

and

$$\rho^\sigma\left(x,t\right)\boldsymbol{u}^\sigma = m^\sigma\sum_i \boldsymbol{e}_i\, f_i^\sigma\left(x,t\right) \tag{2}$$

where m^σ is the molecular mass. For two dimensional D2Q9 model, the equilibrium distribution function can be defined as

$$\begin{aligned} & f_i^{\sigma,eq} = \\ & \rho^\sigma w_i\left[1+\frac{3}{c^2}\boldsymbol{e}_i.\boldsymbol{u}^{\sigma,eq}+\frac{9}{2\,c^4}\left(\boldsymbol{e}_i.\boldsymbol{u}^{\sigma,eq}\right)^2-\frac{3}{2\,c^2}u^{\sigma,eq2}\right] \end{aligned} \tag{3}$$

where w_i is the lattice weighting factors. Therefore the equilibrium velocity becomes

$$\boldsymbol{u}^{eq}=\frac{\sum_\sigma \rho^\sigma\boldsymbol{u}^\sigma/\tau_m^\sigma}{\sum_\sigma \rho^\sigma/\tau_m^\sigma}+\frac{\boldsymbol{F}^\sigma}{2\rho^\sigma} \tag{4}$$

Simultaneously, the lattice Boltzmann energy equation without viscous dissipation for nanofluid defined as [19]

$$\begin{aligned} & g_i^\sigma\left(x+e_i\Delta t, t+\Delta t\right)-g_i^\sigma\left(x,t\right) \\ & =-\frac{1}{\tau_\theta^\sigma}\left(g_i^\sigma\left(x,t\right)-g_i^{\sigma,eq}\left(x,t\right)\right)+\Delta t\, w_i\, G^\sigma \end{aligned} \tag{5}$$

The energy distribution function can be written as

$$\begin{aligned} & g_i^{\sigma,eq} = \\ & \varepsilon^\sigma w_i\left[1+\frac{3}{c^2}\boldsymbol{e}_i.\boldsymbol{u}^{\sigma,eq}+\frac{9}{2c^4}\left(\boldsymbol{e}_i.\boldsymbol{u}^{\sigma,eq}\right)^2-\frac{3}{2c^2}u^{\sigma,eq2}\right] \end{aligned} \tag{6}$$

$\varepsilon^\sigma\left(x,t\right)=\sum_i g_i^\sigma\left(x,t\right)$ is the internal energy variable and $G^\sigma = q^\sigma/\rho^\sigma C_p^\sigma$ is the source or force term per unit time, which is related to the heat generation $\left(q^\sigma\right)$ per unit volume. In the present study, we consider the heat is generated from nanoparticles only, not from base fluid. The mean velocity, temperature, viscosity and thermal diffusivity of the nanofluid can be written as

$$\begin{aligned} & \nu=\left(\sum_\sigma c_m^\sigma\tau_m^\sigma-\frac{1}{2}\right)Cs^2\Delta t, \alpha=\left(\sum_\sigma c_\theta^\sigma\tau_\theta^\sigma-\frac{1}{2}\right)Cs^2\Delta t \\ & \boldsymbol{u}=\frac{\sum_\sigma m^\sigma\sum_i f_i^\sigma\left(x,t\right)\boldsymbol{e}_i}{\sum_\sigma \rho^\sigma}, T=\frac{\sum_\sigma \varepsilon^\sigma\left(x,t\right)}{\sum_\sigma \rho^\sigma C_p^\sigma} \end{aligned} \tag{7}$$

where c_m^σ and c_θ^σ are the concentration of viscosity and diffusivity of each component respectively. Solving the Equations (1) and (5) with other approximations, we

get all information that we interested in our study.

2.2. Numerical Analysis

The physical configuration with boundary conditions for the present study is shown in **Figure 1**. A closed square cavity of length H is considered here. The horizontal walls are assumed to be insulated whereas the vertical walls are maintained at constant but different temperatures T_h (hot) and T_c (cold). For natural convection, the momentum and energy equations are coupled and the flow is driven by temperature or mass gradient, Under Boussinesq approximation, the force term per unit mass can be written as

$$\boldsymbol{F}(\boldsymbol{x},t) = \rho(\boldsymbol{x},t)\, g\, \beta\left(T(\boldsymbol{x},t) - T_{ref}\right)$$

The ratio of the buoyancy force to the product of viscous force and heat diffusion rates defines the Rayleigh number, $\mathrm{Ra} = \mathrm{Pr}\times\mathrm{Gr} = g\beta\Delta TH^3/\alpha\nu$, where Gr is the Grashof number and Pr is the Prandtl number. The boundary conditions are defined as:

$$u = v = \frac{\partial T}{\partial y} = 0 \text{, at } y = 0, H \text{ and } 0 \le x \le L$$

$$T = T_h, u = v = 0 \text{, at } x = 0 \text{ and } 0 \le y \le H$$

$$T = T_c, u = v = 0 \text{, at } x = L \text{ and } 0 \le y \le H$$

2.3. Code Validation

To verify our results with the conventional benchmark and with experimental results, first we consider the cavity is filled with pure fluid like air (Pr = 0.71). It is shown in **Figure 2**. It can be seen from these figures that our present numerical simulation is in very good agreement with numerical results of [3] and experimental solutions of [4]. Moreover, the present LBM also applied for nanofluids and it is necessary to verify our method with other published work. A good agreement is obtained between the present solution and bench mark solution of [3] as illustrated in **Figure 3**. This confirms that our method is correct both for pure and nanofluids.

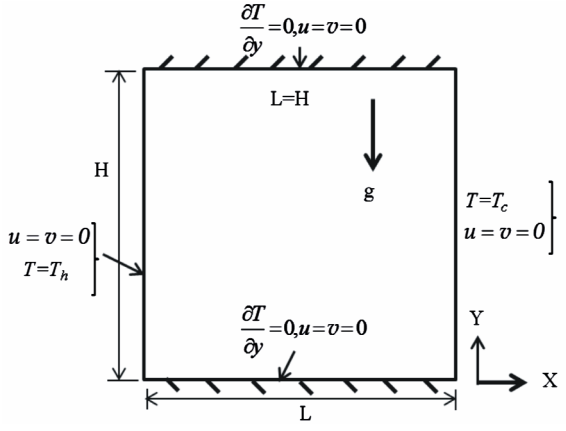

Figure 1. The configuration of the problem under consideration.

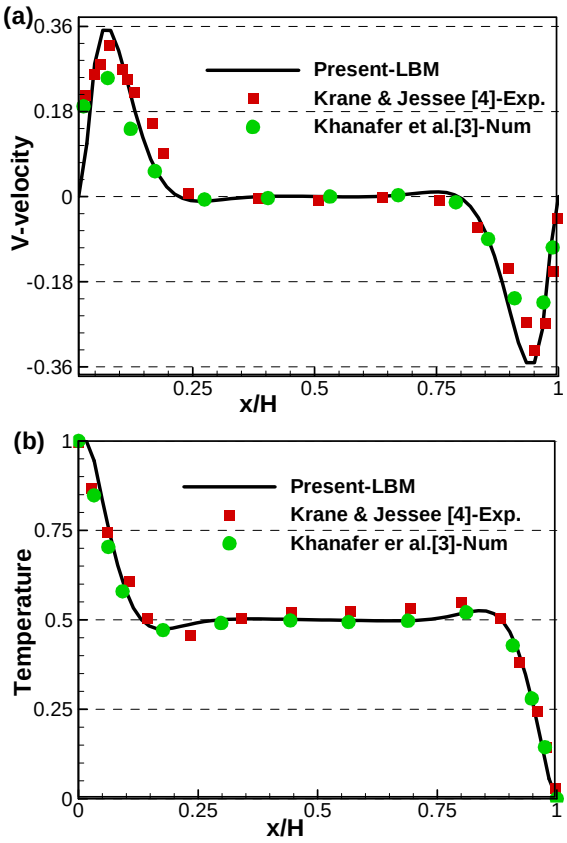

Figure 2. Comparison of dimensionless (a) velocity and (b) temperature profiles for pure fluid (Pr = 0.71, Ra = 1.89 × 10^5).

3. Results and Discussions

Equations (1) and (5) are solved simultaneously on a uniform 2D grid system along with boundary conditions and other equations described in the above sections. Each numerical time step consists of three stages (1) collision, (2) streaming, and (3) boundary conditions steps followed by the LBM approaches. Fluid flow and heat transfer enhancement of nanofluid for a wide range of controlling parameters are discussed in this section. It is assumed that the nanoparticles of Cu are uniformly suspended in water; there is no aggregation of nanoparticles in the fluid medium.

The computed velocity field in the buoyancy driven cavity flow for pure and nanofluids are seen in **Figures 4(a)** and **(b)** respectively. The arrows denote the velocity vectors in both magnitude and direction and the solid lines represent the stream lines of H_2O-Cu nanofluid. The general magnitude of the velocity can be seen to increase as the hot fluid, near the hot wall, flow upward and the

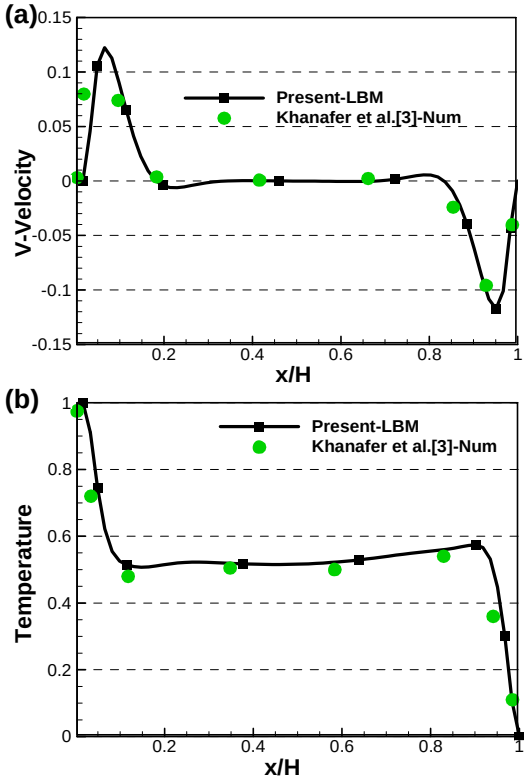

Figure 3. Comparison of velocity and temperature profiles for nanofluid (Pr = 6.2, Gr = 10^5, ϕ = 10%).

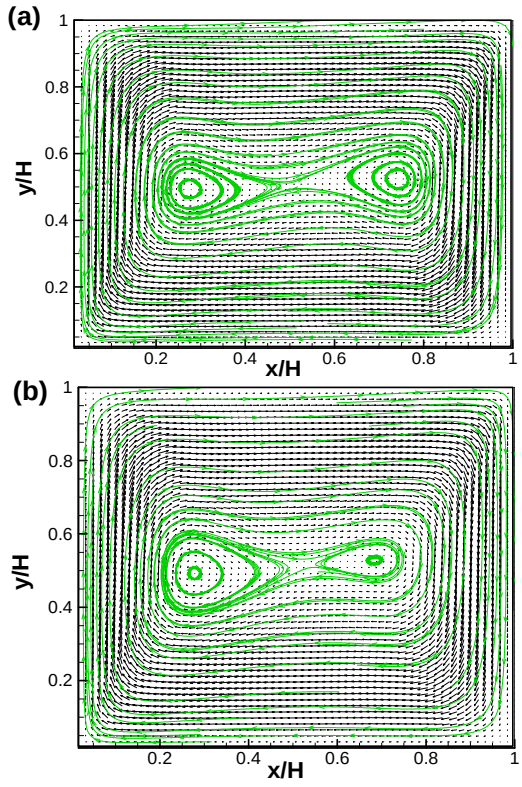

Figure 4. Velocity vectors and stream lines for (a) pure fluid (H_2O) and (b) nanofluid (H_2O-Cu).

cold fluid, near the cold wall, flow downward due to the effect of buoyancy force for both pure and nanofluids. It is one of the main criteria of natural convection in a differently heated cavity. Thus it is clear that the nanofluids flow behavior like a pure fluid.

The effect of internal heat generation of nanoparticles on the velocity and temperature fields at the mid section of the cavity for different particle diameters and volume fractions are illustrated in **Figures 5** and **6**.

It is seen from **Figure 5(a)** that the velocity profiles of nanofluid decrease remarkably with increasing the particle diameter near hot wall and increase near the cold wall. But, in presence of internal heat generation of nanoparticles (dashed lines, **Figure 5(a)**), the velocity profiles near the hot and cold walls have shown infinitesimal changed, decreased (zoom viewed) near hot wall. It is also seen that the location of the local maximum and minimum for all cases have tend to moved to right from hot wall and left from cold wall with increasing the particle diameter. For dp = 5 nm, the local maximum and minimum are seen at approximately x/H = 0.06 and x/H = 0.85, whereas for dp = 10 and 20 nm, the locations are observed at x/H = 0.09 and x/H = 0.93; and x/H = 0.10 and x/H = 0.90 respectively. These represented that the velocity boundary layer become thicker with increasing particle diameters.

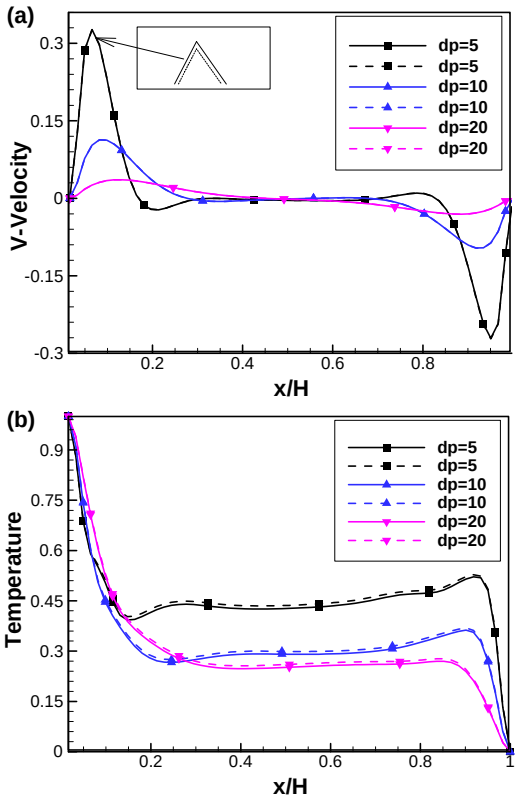

Figure 5. (a) Dimensionless velocity and (b) temperature profiles for different particle diameters (nm) (solid lines: no heat generation, dashed lines: with heat generation).

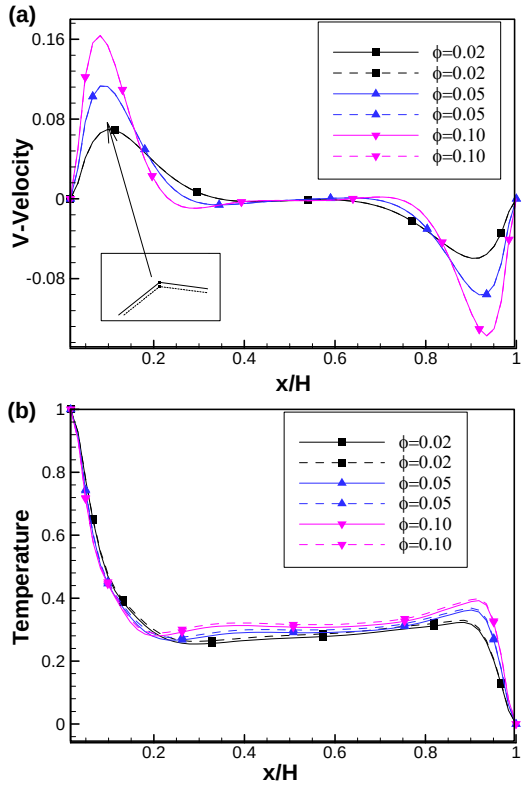

Figure 6. (a) Dimensionless velocity and (b) temperature profiles for different particle volume fractions (%) (solid lines: no heat generation, dashed lines: with heat generation).

From **Figure 5(b)**, it is observed that, the temperature profiles increase slightly near the hot wall but decrease significantly throughout the cavity with increasing the particle diameters and finally satisfied the boundary conditions. Moreover, in presence of heat generation, dased lines in **Figure 5(b)**, the temperature profiles slightly increased compare to without heat generation. It means that, if the nanoparticles generate the heat, the particle lost some energy to the fluid and consequently the average temperature of nanofluid increased. From **Figure 5 (b)**, the significant temperature gradient observed in the vicinity of the heated surface approximately, $0 \le x/H \le 0.15$, and unheated surface $0.95 \le x/H \le 1$ for $dp = 5$ nm; $0 \le x/H \le 0.22$ and $0.92 \le x/H \le 1$ for $dp = 10$ nm; $0 \le x/H \le 0.28$ and $0.88 \le x/H \le 1$ for $dp = 20$ nm. Therefore, it is seen that thermal stratification and increase in temperature in the direction of heat flow in the core region respectively $0.15 < x/H < 0.95$, $0.22 < x/H < 92$ and $0.28 < x/H < 0.88$ for $dp = 5$ nm, 10 nm and 20 nm. This indicates that thermal boundary layer increased with increasing particle diameters.

The effects of volume fractions with internal heat generation of nanoparticles on fluid flow are shown in **Figure 6**. It is shown that the velocity profiles of nanofluid increases remarkably with volume fractions of nanofluid near hot wall and decreased near cold wall. In more details, the velocity along the vertical walls of the cavity show a higher level of activity as predicted by thin layer of hydrodynamic velocity boundary layers. Whereas, the variation of the velocity at the center of the cavity for all volume fractions of nanoparticles are negligible compared with those of boundaries in all cases. This is expected as the maximum fluid motion at the boundaries and almost stagnant in the core region. The locations of the local maximum and minimum velocities for all cases are approximately at the same position of $X(=x/H)$. The effect of dimensionless temperature profiles with increase of volume fractions at the centerline of the cavity, which is perpendicular direction of the heated walls of the cavity, as shown in **Figure 6(b)**. The variation of temperature near hot and cold walls versus dimensionless horizontal length is linear for all volume fractions, which is the characteristic of heat transfer by convection. For all values of ϕ, a significant temperature gradient is observed in the vicinity of the heated surface approximately, $0 \le x/H \le 0.22$, and unheated surface $0.92 \le x/H \le 1$. Moreover, it is seen that thermal stratification and increase in temperature in the direction of heat flow in the core region $0.22 < x/H < 0.92$. In physical meaning, the temperature should decrease in the direction of heat flow, but for natural convection in a cavity, the rate of cooling is expected to be higher near the heated and unheated walls due to the fluid motion and hydrodynamics effects. This phenomenon is attributed to buoyancy-induced cellular flows in the boundary layer adjoining the heated and cold walls. The fluid motion increases the rate of heat transfer.

A usual means of characterizing heat transfer is to calculate the Nusselt number. Actually the Nusselt number Nu is a dimensionless form of the heat transfer coefficient. To investigate the heat transfer performance in terms of effective thermal conductivity of the nanofluid, the local Nusselt number Nu_L and the averaged Nusselt number Nu over the flow channel are respectively defined as follows:

$$Nu_L = \frac{hH}{k_f} \tag{8}$$

The heat transfer coefficient h is defined as

$$h = \frac{q_w}{T_h - T_c}, \quad q_w = -k_{nf}\frac{\partial T}{\partial x} \tag{9}$$

Here T_h and T_c are the temperature of heated and cooled walls respectively. The heat flux, q_w, of nanofluid can be expressed in terms of thermal conductivity K_{nf} of nanofluid, k_f are the thermal conductivity of the base fluid and H is the channel height. The Nusselt number and the average Nusselt number in dimensionless form on the left heated wall are defined as

$$Nu = \int_0^1 Nu_L(Y)\,dY,\ Nu_L(Y) = -\frac{k_{nf}}{k_f}\left(\frac{\partial\theta}{\partial X}\right)_{wall} \quad (10)$$

where, θ, is the non-dimensional temperature. On the basis of the definition [5], the effective thermal conductivity for a two-component mixture (Cu-H_2O) is defined as

$$k_{nf} = \alpha_{nf}\left(\rho C_p\right)_{nf} \quad (11)$$

The average Nusselt number and the thermal conductivity ratios for constant Rayleigh number, Ra = 10^5 at 100,000 time steps with various volume fractions and particle diameters as well as the internal heat generation of nanoparticles are shown in **Figures 7** and **8**.

The dimensionless rate of heat transfer called Nusselt number (Nu) is significantly decreased with increasing the particle diameters from *dp* = 5 nm to 40 nm, as described in **Figure 7(a)**, though it is increased with particle volume fractions. Moreover, it is observed that in presence of nanoparticles heat generation, the Nusselt number slightly decreases (dashed lines) compare to without heat generation (solid lines). Similar phenomenon is seen for thermal conductivity ratio. It is seen

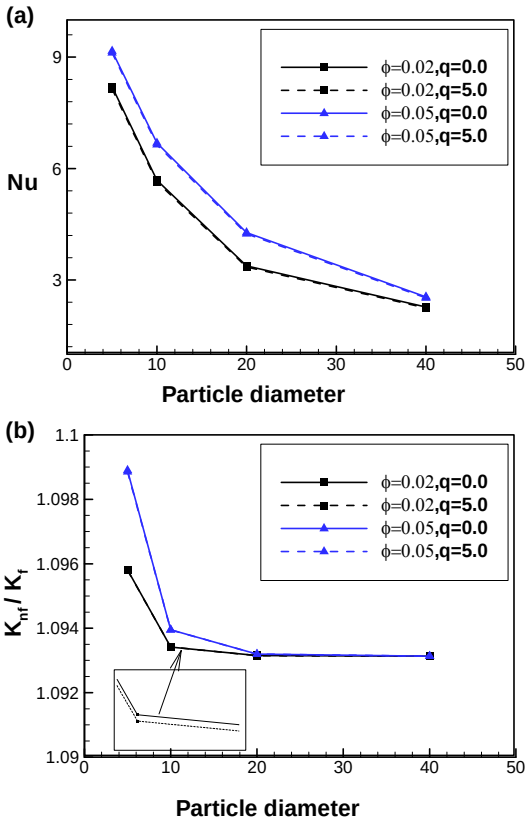

Figure 7. (a) The average rate of heat transfer (Nusselt number, Nu); (b) Thermal conductivity ratios for different particle diameters (solid lines: no heat generation, dashed lines: with heat generation).

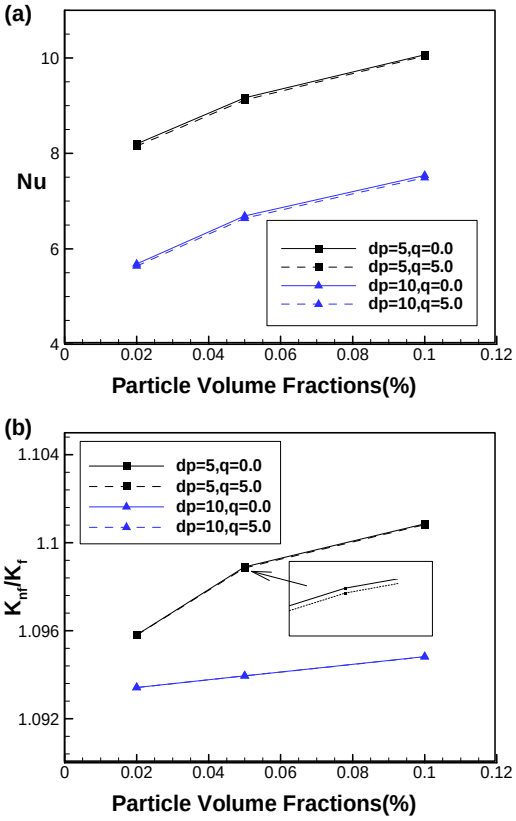

Figure 8. (a) The average rate of heat transfer (Nusselt number, Nu); (b) Thermal conductivity ratios for different particle volume fraction s (%) (solid lines: no heat generation, dashed lines: with heat generation).

almost constant for *dp* > 30 nm for all cases. This is because constant Rayleigh number effect. In natural convection flow, the thermal conductivity is strongly dependent on the Rayleigh number.

It can be seen from **Figure 8** that both of the measured dimensionless rate of heat transfer in terms of Nusselt number and the thermal conductivity are increased with increased of volume fractions. This increased is significantly depending on particle size. For increasing particle diameter both of the heat transfer characteristics are dramatically decreased. With the heat generation of nanoparticles, it is also observed that both of heat transfer rate and conductivity ratio decreases very slightly.

Actually, in the above cases, the particle size is important factor. The large size of particle diameter means that the less number of particles. Therefore, the surface area of nanoparticle decreases, giving less heat transfer area between the phases. In natural convection flow, only buoyancy force is a dominant force, therefore, particle movement is very important. The main problem for large size of particle is the rapid settling in the fluid. Other problems are abrasion and clogging. These problems are highly undesirable for many practical cooling industries.

4. Conclusions

The Thermal Lattice-Boltzmann Method (TLBM) is successfully applied in this work to simulate buoyancy-driven heat transfer characteristics and flow performance of Cu-H_2O nanofluid in a square cavity. Throughout our calculation, it is assumed that constant Rayleigh number, $Ra = 10^5$. So the fluid flow and heat transfer analysis are depending on particle size and volume fractions. Moreover, it is considered that the internal heat generation effect of nanoparticles to the base fluid, and then finally, we have shown our result of the resultant fluid called nanofluid. The present results indicate that the following statements:

- Both of the thermal boundary layer and velocity boundary layer thickness increased with increasing the particle diameter. However, the change of thickness of thermal and velocity boundary layers are negligible with increasing the particle volume fractions within the range up to 10%.
- The heat transfer features, the heat transfer rate and the thermal conductivity ratio, of a nanofluid are increased with increase of the nanoparticle volume fractions.
- However, the rate of heat transfer and thermal conductivity ratio are significantly decreased with increase of particle diameter.
- In addition, all of the above features are very slightly changed (decreased) with internal heat generation effect of nanoparticle due to the constant Rayleigh number and Prandtl number at the present study.
- For small particle diameter, the nanofluid behaves more like a fluid than the conventional solid-fluid mixer. The results from our analysis have shown quite good and this temperature characteristic enhancement plays a significant role in engineering applications such as in the electronic cooling industries or MEMS devices.

REFERENCES

[1] S. Lee, S. U.-S. Choi, S. Li and J. A. Eastman, "Measuring Thermal Conductivity of Fluids Containing Oxide Nanoparticles," *Journal of Heat Transfer*, Vol. 121, No. 2, 1999, pp. 280-289.

[2] Y. Xuan and Q. Li, "Heat Transfer Enhancement of Nanofluids," *International Journal of Heat and Fluid Flow*, Vol. 21, No. 1, 2000, pp. 58-64. doi:10.1016/S0142-727X(99)00067-3

[3] K. Khanafer, K. Vafai and M. Lightstone, "Buoyancy-Driven Heat Transfer Enhancement in a Two-Dimensional Enclosure Utilizing Nanofluids," *International Journal of Heat and Mass Transfer*, Vol. 46, No. 19, 2003, pp. 3639-3653. doi:10.1016/S0017-9310(03)00156-X

[4] R. Krane and J. Jessee, "Some Detailed Field Measurement for a Natural Convection Flow in a Vertical Square Enclosure," *Proceedings of the First ASME-JSME Thermal Engineering Joint Conference*, Honolulu, 20-24 March 1983, pp. 323-329.

[5] S. K. Das, S. U.-S. Choi, W. Yu and T. Pradeep, "Nanofluids, Science and Technology," Wiley Interscience, Hoboken, 2007.

[6] M. A. Taher, "Fluid Flow and Heat Transfer Analysis of Pure and Nanofluids Using Lattice-Boltzmann Method," Ph.D. Thesis, Pukyong National University, Busan, 2009.

[7] W. Yu, D. M. France, J. L. Routbort and S. U.-S. Choi, "Review and Comparison of Nanofluid Thermal Conductivity and Heat Transfer Enhancements," *Heat Transfer Engineering*, Vol. 29, No. 29, 2008, pp. 432-460. doi:10.1080/01457630701850851

[8] X. Shan and H. Chen, "Lattice Boltzmann Model for Simulating Flows with Multiple Phases and Components," *Physical Review E*, Vol. 47, No. 3, 1993, pp. 1815-1820. doi:10.1103/PhysRevE.47.1815

[9] M. A. Taher and Y. W. Lee, "Numerical Study on Reduction of Fluid Forces Acting on a Circular Cylinder with Different Control Bodies Using Lattice-Boltzmann Method," *International Journal of Energy & Technology*, Vol. 4, No. 18, 2012, pp. 1-7.

[10] M. A. Taher**,** S. C. Saha, Y. W. Lee and H. D. Kim, "Numerical Study of Lid-Driven Square Cavity with Heat Generation Using LBM," *American Journal of Fluid Dynamics*, Vol. 3, No. 2, 2013, pp. 40-47. doi:10.5923/j.ajfd.20130302.04

[11] A. A. Mohammad, "Applied Lattice Boltzmann Method for Transport Phenomena, Momentum, Heat and Mass Transfer," The University of Calgary, Calgary, 2007.

[12] S. Succi, "The Lattice Boltzmann Equation for Fluid Dynamics and beyond," Oxford University Press, Oxford, 2001.

[13] X. Shan, "Simulation of Rayleigh-Bernard Convection Using Lattice Boltzmann Method," *Physical Review E*, Vol. 55, No. 3, 1997, pp. 2780-2788. doi:10.1103/PhysRevE.55.2780

[14] M. A. Taher, K.-M. Li and Y.W. Lee, "Numerical Study of H_2O-Cu Nanofluid Using Lattice-Boltzmann Method," *Journal of the Korean Society of Marine Engineering*, Vol. 34, No. 1, 2010, pp. 53-61. doi:10.5916/jkosme.2010.34.1.053

[15] A. K. Santa, S. Sen and N. Chakraborti, "Study of Heat Transfer Augmentation in a Differentially Heated Square Cavity Using Copper-Water Nanofluid," *International Journal of Thermal Sciences*, Vol. 47, No. 9, 2008, pp. 1113-1122. doi:10.1016/j.ijthermalsci.2007.10.005

[16] J. Cai, X. Huai, R. Yan and Y. Cheng, "Numerical Simulation on Enhancement of Natural Convection Heat Transfer by Acoustic Cavitation in a Square Enclosure," *Applied Thermal Engineering*, Vol. 29, No. 10, 2009, pp. 1973-1982. doi:10.1016/j.applthermaleng.2008.09.015

[17] S. Sivasankaran, T. Asaithambi and S. Rajan, "Natural Convection of Nanofluids in a Cavity with Linearly Varying Wall Temperature," *Maejo International Journal of Science and Technology*, Vol. 4, No. 3, 2010, pp. 468-482.

[18] J. M. Buick and C. A. Greated, "Gravity in Lattice Boltzmann Model," *Physical Review E*, Vol. 61, No. 5, 2000, pp. 5307-5320. doi:10.1103/PhysRevE.61.5307

[19] Y. Xuan and Z. Yao, "Lattice Boltzmann Model for Nanofluids," *Heat Mass Transfer*, Vol. 41, No. 3, 2005, pp. 199-205. doi:10.1007/s00231-004-0539-z

[20] N. S. Martys and H. Chen, "Simulation of Multicomponent Fluids in Complex Three-Dimensional Geometries by the Lattice Boltzmann Method," *Physical Review E*, Vol. 53, No. 1, 1996, pp. 743-750. doi:10.1103/PhysRevE.53.743

[21] Y. M. Xuan, K. Yu and Q. Li, "Investigations of Flow and Heat Transfer of Nanofluids by the Thermal Lattice-Boltzmann Model," *Progress in Computational Fluid Dynamics*, Vol. 5, No. 1-2, 2005, pp. 13-19.

